ROM2F/2002/12 (May 2002) to appear in the Proceed. of DARK2002.

WIMP Search by DAMA at Gran Sasso

R. Bernabei[1], M. Amato[2], P. Belli[1], F. Cappella[1], R. Cerulli[1], C.J. Dai[3], H.L. He[3], G. Ignesti[2], A. Incicchitti[2], H.H. Kuang[3], J.M. Ma[3], F. Montecchia[1], F. Nozzoli[1], and D. Prosperi[2]

[1] Dip.to di Fisica, Università di Roma "Tor Vergata" and INFN, sez. Roma2, I-00133 Rome, Italy
[2] Dip.to di Fisica, Università di Roma "La Sapienza" and INFN, sez. Roma, I-00185 Rome, Italy
[3] IHEP, Chinese Academy, P.O. Box 918/3, Beijing 100039, China.

Abstract. DAMA is searching for rare processes by developing and using several kinds of radiopure scintillators: in particular, NaI(Tl), liquid Xenon and CaF_2(Eu). Here only the results released so far on the WIMP annual modulation signature are summarized and compared with results from other experiments, including the recent re-analysis of CDMS-I data. Next perspectives are also shortly addressed.

1 Introduction

DAMA is devoted to the search for rare processes (such as WIMPs direct detection, $\beta\beta$ processes, charge-non-conserving processes, Pauli exclusion principle violating processes, nucleon instability, solar axions and exotics [1,2,3,4,5,6,7,8,9,10,11,12]) by developing and using low radioactive scintillators. The main experimental set-ups, which are running at present, are: the $\simeq$ 100 kg NaI(Tl) set-up, the $\simeq$ 6.5 kg liquid Xenon (LXe) set-up and the so-called "R&D" apparatus. Moreover, a low-background germanium detector is operative underground since many years for measurements and selections of samples.

In this paper only the results obtained in the search for WIMPs by exploiting the annual modulation signature with the $\simeq$ 100 kg NaI(Tl) set-up, their comparison with those of other experiments (including the more recent re-analysis of the CDMS-I data) and some perspectives of the new LIBRA (Large sodium Iodine Bulk for RAre processes) set-up in preparation will be addressed.

A full description of the $\simeq$ 100 kg NaI(Tl) set-up and of its performances can be found in ref.[5]. It is worth to note that some upgrading has been performed since then; in particular, during August 2000 the electronic chain and the DAQ have been fully substituted achieving improved performances.

The recoil/electron light ratio for ^{23}Na and ^{127}I and the pulse shape discrimination capability have been measured by neutron source and upper limits on recoils have been measured in this set-up by exploiting the pulse shape discrimination technique [3]. Moreover, studies on possible diurnal variation of the low

energy rate in the data of the $\simeq$ 100 kg NaI(Tl) set-up have also been carried out. It could be expected because of the Earth's daily rotation; in fact, during the sidereal day the Earth shields a given detector with a variable thickness, eclipsing the "wind" of Dark Matter particles but only in case of high cross section candidates (to which small halo fraction would correspond). By analyzing a statistics of 14962 $kg \times day$ no evidence for diurnal rate variation with sidereal time has been observed [2]; this result supports that the effect pointed out by the studies on the WIMP annual modulation signature (see later) would account for a halo fraction $\gtrsim 10^{-3}$ [2].

The main goal of the $\simeq$ 100 kg NaI(Tl) set-up is to investigate the WIMP annual modulation signature. In fact, the WIMPs are embedded in the galactic halo; thus, our solar system, which is moving with respect to the galactic system, is continuously hit by a WIMP "wind" which can be mainly searched for by WIMP elastic scattering on the target nuclei of the detector. In particular, since the Earth rotates around the Sun, which is moving with respect to the galactic system, it would be crossed by a larger WIMP flux in June (when its rotational velocity is summed to the one of the solar system with respect to the Galaxy) and by a smaller one in December (when the two velocities are subtracted). The fractional difference between the maximum and the minimum of the rate is expected to be of order of $\simeq$ 7%.

The $\simeq$ 100 kg highly radiopure NaI(Tl) DAMA set-up [5] can effectively exploit such a signature because of its well known technology, of its high intrinsic radiopurity, of its mass, of its suitable control of all the operational parameters and of the deep underground experimental site.

The annual modulation signature is very distinctive as we have already pointed out [4,5,6,7,8,9,10,11]. In fact, a WIMP-induced seasonal effect must simultaneously satisfy all the following requirements: the rate must contain a component modulated according to a cosine function (1) with one year period (2) and a phase that peaks around $\simeq 2^{nd}$ June (3); this modulation must be found in a well-defined low energy range, where WIMP induced recoils can be present (4); it must apply to those events in which just one detector of many actually "fires", since the WIMP multi-scattering probability is negligible (5); the modulation amplitude in the region of maximal sensitivity must be $\lesssim$7% (6). Only systematic effects able to fulfil these 6 requirements could fake this signature; no one able to do that has been found or suggested [9], on the contrary of what sometimes claimed by some author (see eg. ref. [13]).

Results obtained by investigating the annual modulation signature in the data collected during the first four annual cycles have been released so far [4,6,7,8,9,10,11]. The latter ones are summarized below and compared with those of some other experiments. At present the experiment is running taking data for the 7^{th} cycle; at the end of this cycle the new LIBRA set-up ($\simeq$ 250 kg of NaI(Tl)) will be installed.

2 A Model Independent Analysis of the Annual Modulation Data

The annual modulation signature offers the possibility to obtain a model independent evidence for the presence of a WIMP component in the galactic halo. The large number of peculiarities (see above), which have to be satisfied for that, assures the absence of possible known systematic effects able to mimic such a signature (see above and ref. [9]) and, therefore, an effective tool of investigation, as originally pointed out in ref. [14].

The data released so far refer to a total statistics of 57986 $kg \cdot day$ collected during four independent experiments of one year cycle each one. A model independent analysis of these data offers an immediate evidence of the presence of an annual modulation of the rate of the single hit events in the lowest energy interval (2 – 6 keV) as shown in Fig. 1. There each data point has been obtained from the raw rate measured in the corresponding time interval, after subtracting the constant part. The results of the four years give consistent results with

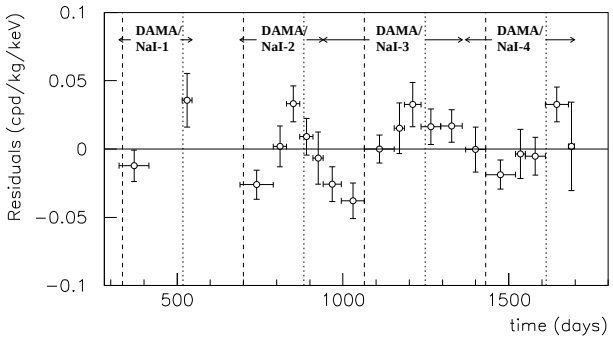

Fig. 1. Model independent residual rate for single hit events, in the 2–6 keV cumulative energy interval, as a function of the time elapsed since January 1-st of the first year of data taking. The expected behaviour of a WIMP signal is a cosine function with minimum roughly at the dashed vertical lines and with maximum roughly at the dotted ones.

proper period and phase. In particular, the χ^2 test on the data of Fig. 1 disfavors the hypothesis of unmodulated behaviour (probability: $4 \cdot 10^{-4}$). No modulation is found in higher energy regions.

We have extensively discussed the results of the investigations of all the possible known systematics when releasing the data of each annual cycle; moreover, a dedicated paper [9] has been released on this topic. No known systematic effect or side reaction able to mimic a WIMP induced effect has been found as discussed in details in ref. [9]. In particular, no effect mentioned in ref. [13] can be able to mimic it (see e.g. ref. [9]).

In conclusion, a WIMP contribution to the measured rate is candidate by the result of the model independent approach independently on the nature and coupling with ordinary matter of the possible WIMP particle.

3 Model Dependent Analyses of the Annual Modulation Data

To investigate the nature and coupling with ordinary matter of a possible candidate, a suitable energy and time correlation analysis is necessary as well as a complete model framework. We remark that a model framework is identified not only by general astrophysical, nuclear and particle physics assumptions, but also by the set of values used for all the parameters needed in the model itself and in related quantities (for example WIMP local velocity, v_0, form factor parameters, etc.).

For simplicity, initially we have considered the case of purely spin-independent coupled WIMP. In fact, often the spin-independent interaction with ordinary matter is assumed to be dominant since e.g. most of the used target-nuclei are practically not sensitive to SD interactions as on the contrary ^{23}Na and ^{127}I are and the theoretical calculations are even more complex.

Moreover, the simplest model scenario has been considered as well as fixed parameters values [4,6]. Then, this case has been extended by considering the many uncertainties which exist on the astrophysical velocity distribution [7,8] and the physical constraint which arises from the measured upper limits on recoils [8]. Then, some of the other possible particle scenarios have been considered such as extensions to the general case of WIMPs with both spin-independent (SI) and spin-dependent (SD) coupling [10] and to that of WIMPs with inelastic scattering [11]. In these latter cases, the effect of the uncertainties on some other parameters has been included. Moreover, recently an investigation on the effect induced by different consistent halo models on the result for purely SI coupled WIMPs has also been carried out in ref. [12].

At present the lightest supersymmetric particle named neutralino is considered the best candidate for WIMP. Note, in particular, that the results of the data analyses [8,10,11] summarized here and in the following hold for the neutralino, but are not restricted only to this candidate.

In supersymmetric theories both the squark and the Higgs bosons exchanges give contribution to the coherent (SI) part of the neutralino cross section, while the squark and the Z^0 exchanges give contribution to the spin dependent (SD) one. Therefore, the differential energy distribution of the recoil nuclei in WIMP-nucleus elastic scattering can be calculated [3,15] by means of the differential cross section of the WIMP-nucleus elastic processes: $\frac{d\sigma}{dE_R}(v, E_R) = \left(\frac{d\sigma}{dE_R}\right)_{SI} + \left(\frac{d\sigma}{dE_R}\right)_{SD}$ where v is the WIMP velocity in the laboratory frame and E_R is the recoil energy.

3.1 WIMPs With Dominant SI Interaction in a Given Model Framework

As first scenario a full energy and time correlation analysis – properly accounting for the physical constraint arising from the measured upper limit on recoils

[3,9] – has been carried out in the framework of a given model for purely spin-independent coupled candidates with mass above 30 GeV. A standard maximum likelihood method has been used. Following the usual procedure we have built the y log-likelihood function, which depends on the experimental data and on the theoretical expectations for the considered model framework; then, y is minimized and parameters' regions allowed at given confidence level are derived. Note that different model frameworks (see above) vary the expectations and, therefore, the cross section and mass values corresponding to the y minimum, that is also the allowed region at given C.L.. In particular, the inclusion of the uncertainties associated to the models and to every parameter in the models themselves as well as other possible scenarios largely enlarges the allowed region as discussed e.g. in ref. [7] for the particular case of the astrophysical velocities. In the case considered in ref. [8] the minimization procedure has been repeated by varying the WIMP local velocity, v_0, from 170 km/s to 270 km/s to account for its present uncertainty. For example, the values $m_W = (72^{+18}_{-15})$ GeV and $\xi\sigma_{SI} = (5.7 \pm 1.1) \cdot 10^{-6}$ pb correspond to the position of y minimum when v_0 = 170 km/s, while $m_W = (43^{+12}_{-9})$ GeV and $\xi\sigma_{SI} = (5.4 \pm 1.0) \cdot 10^{-6}$ pb when $v_0 = 220$ km/s. Here, ξ is the WIMP local density in 0.3 GeV cm^{-3} unit, σ_{SI} is the point-like SI WIMP-nucleon generalized cross section and m_W is the WIMP mass. Fig. 2 shows the regions allowed at 3σ C.L. in such a model framework, when the uncertainty on v_0 is taken into account (solid contour) and when pos-

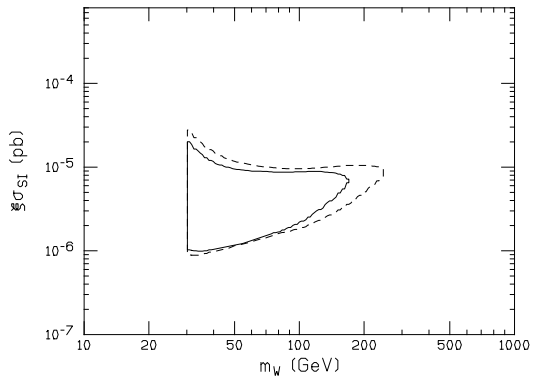

Fig. 2. A purely SI case: regions allowed at 3σ C.L. on the plane $\xi\sigma_{SI}$ versus m_W for a WIMP with dominant SI interaction and mass above 30 GeV in the model framework considered in ref. [8]: i) when v_0 uncertainty (170 km/s $\leq v_0 \leq$ 270 km/s; continuous contour) has been included; ii) when also a possible bulk halo rotation as in ref. [7] (dashed contour) is considered. Note that these regions hold for the given model framework (assumptions and parameters) and correspond to the superposition of all the 3 σ allowed regions obtained when varying v_0 in the allowed range; thus many "most likely" values correspond to it. Moreover, as widely known, the inclusion of present uncertainties on some other astrophysical, nuclear and particle physics parameters would enlarge these regions (varying again consequently the "most likely" values for each considered set). Some partial discussions can be found in [7,8,12].

sible bulk halo rotation is considered (dashed contour). For simplicity, no other uncertainty on the used parameters has been considered there (some of them have been included in the approach summarized in the next subsection [10]); thus, obviously the real allowed region including the effect of all the uncertainties is much larger than quoted for this simplified model framework as discussed at some extent also in ref. [8] and recently shown – as regards the halo model effect – in ref. [12] (see Fig. 3).

A quantitative comparison between the residuals and the modulation amplitudes for this particular model framework has been discussed in ref. [8]. Moreover, we remark that the energy and time behaviour of the modulation amplitudes and residuals as well as the accounting for known uncertainties (such as quenching factors, form factors parameters, etc.) play a crucial role to obtain a meaningful comparison.

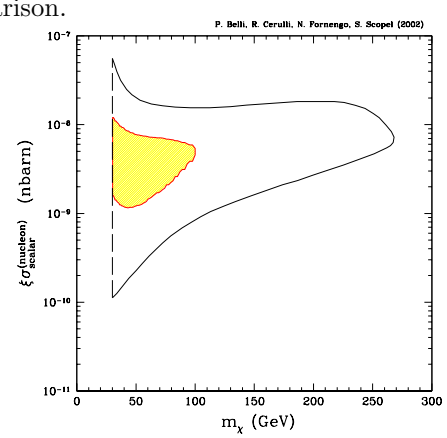

Fig. 3. Effect of halo modelling: the external continuous contour is the 3σ annual modulation region for purely SI coupled WIMPs in the plane $\xi\sigma_{SI}$ (where $\sigma_{SI} = \sigma^{(nucleon)}_{scalar}$) versus WIMP mass, obtained by considering all the (non-rotating) galactic halo models discussed in ref. [12]. To point out the effect of the halo modelling alone, there is also shown the internal dashed region which corresponds to a simplified model of isothermal galactic halo in the same framework as ref. [8], but assuming here the v_0 value at 220 km/s.

In conclusion, the observed effect investigated in terms of a WIMP candidate with dominant SI interaction and mass above 30 GeV in the simplified model framework considered in ref. [8], supports allowed WIMP masses up to about 105 GeV (1 σ C.L.) and even up to about 250 GeV (1 σ C.L.) if different halo models are considered [12]. Lower $\xi\sigma_{SI}$ would be implied by the inclusion of known uncertainties on parameters (for example, on the quenching factors and on the form factor parameters) and on model features.

Theoretical implications of these results in terms of a neutralino with dominant SI interaction and mass above 30 GeV have been discussed in ref. [15,16], while the case for an heavy neutrino of the fourth family has been considered in ref. [17]. Let us comment that a correct evaluation and interpretation of the theoretical results are necessary; in fact, sometimes the uncertainties on the local

halo density are not taken into account and the rescaling procedures are not often applied to correctly evaluate the WIMP local density. They must be considered for a reliable and correct presentation as well as the uncertainties which exist on some aspects of supersymmetric models in order to avoid that the given figure "would drive" the reader to wrong conclusion. Finally, note that the density of points in the calculated scatter plots do not represent a probability density.

3.2 WIMPs With Mixed Coupling in Given Model Framework

Since the ^{23}Na and ^{127}I nuclei are sensitive to both SI and SD couplings – on the contrary e.g. of ^{nat}Ge and ^{nat}Si which are sensitive mainly to WIMPs with SI coupling (only 7.8 % is non-zero spin isotope in ^{nat}Ge and only 4.7% of ^{29}Si in ^{nat}Si) – the analysis of the data has been extended considering the more general case [10]. This implies a WIMP having not only a spin-independent, but also a spin-dependent coupling different from zero, as it is also possible e.g. for the neutralino.

Then, the log-likelihood function has been minimized – properly accounting also for the physical constraint set by the measured upper limit on recoils [3] – and parameters' regions allowed at given confidence level have been obtained. In particular, the calculation has been performed by minimizing the y function with respect to the $\xi\sigma_{SI}$, $\xi\sigma_{SD}$ and m_W parameters for each given θ value. Here, σ_{SD} is the point-like SD WIMP cross section on nucleon and $tg\theta$ is the ratio between the effective SD coupling constants on neutrons, a_n, and on proton, a_p; therefore, θ can assume values between 0 and π depending on the SD coupling. In the present framework the uncertainties on v_0 have been included; moreover, the uncertainties on the nuclear radius and the nuclear surface thickness parameter in the SI form factor, on the b parameter in the used SD form factor and on the measured quenching factors [3] of these detectors have also been considered [10]. For simplicity, Fig. 4 shows slices for some m_W of the region allowed at 3 σ C.L. in the ($\xi\sigma_{SI}$, $\xi\sigma_{SD}$, m_W) space for four particular couplings: i) $\theta = 0$ (a_n =0 and $a_p \neq 0$ or $|a_p| >> |a_n|$); ii) $\theta = \pi/4$ ($a_p = a_n$); iii) $\theta = \pi/2$ ($a_n \neq 0$ and a_p = 0 or $|a_n| >> |a_p|$); iv) $\theta = 2.435$ rad ($\frac{a_n}{a_p}$ = -0.85, pure Z^0 coupling). The case $a_p = -a_n$ is nearly similar to the case iv).

As already pointed out, when the SD contribution goes to zero (y axis in Fig. 4), an interval not compatible with zero is obtained for $\xi\sigma_{SI}$. Similarly, when the SI contribution goes to zero (x axis in Fig. 4), finite values for the SD cross section are obtained. Large regions are allowed for mixed configurations also for $\xi\sigma_{SI} \lesssim 10^{-5}$ pb and $\xi\sigma_{SD} \lesssim 1$ pb; only in the particular case of $\theta = \frac{\pi}{2}$ (that is $a_p = 0$ and $a_n \neq 0$) $\xi\sigma_{SD}$ can increase up to $\simeq 10$ pb, since the ^{23}Na and ^{127}I nuclei have the proton as odd nucleon. Moreover, in ref. [10] we have also pointed out that: i) finite values can be allowed for $\xi\sigma_{SD}$ even when $\xi\sigma_{SI} \simeq 3 \cdot 10^{-6}$ pb as in the region allowed in the pure SI scenario considered in the previous subsection; ii) regions not compatible with zero in the $\xi\sigma_{SD}$ versus m_W plane are allowed even when $\xi\sigma_{SI}$ values much lower than those allowed in the dominant SI scenario previously summarized are considered; iii) minima of the y function

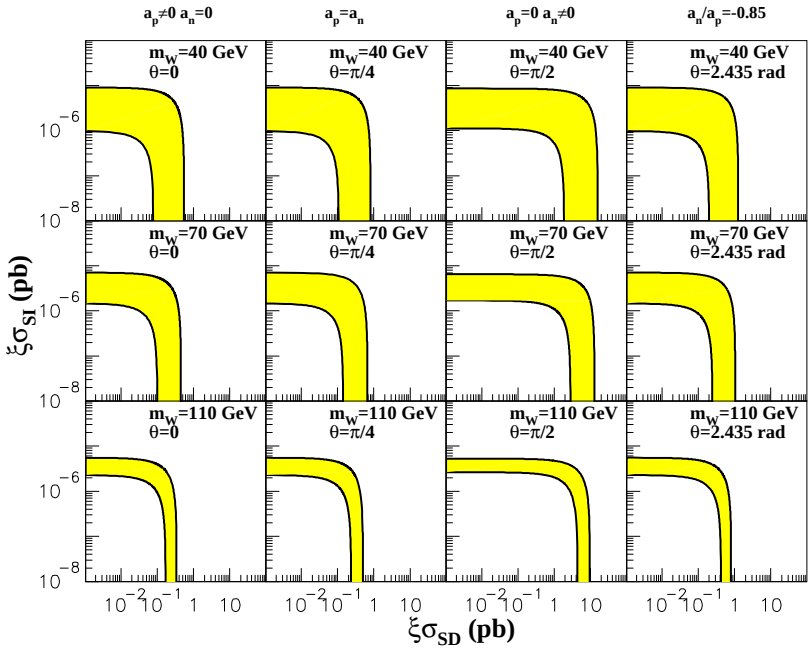

Fig. 4. A mixed SI/SD case: example of slices of the region allowed at 3 σ C.L. in the ($\xi\sigma_{SI}$, $\xi\sigma_{SD}$, m_W) space for some m_W and θ values in the model framework considered in ref. [10]. Only four particular couplings are reported here for simplicity: i) $\theta = 0$; ii) $\theta = \pi/4$ iii) $\theta = \pi/2$; iv) $\theta = 2.435$ rad. Note that e.g. Ge experiments are sensitive mainly only to SI coupling and, therefore, cannot explore most of the DAMA allowed regions in this scenario.

with both $\xi\sigma_{SI}$ and $\xi\sigma_{SD}$ different from zero are present for some m_W and θ pairs; the related confidence level ranges between $\simeq 3\ \sigma$ and $\simeq 4\ \sigma$ [10].

Further investigations are in progress on these model dependent analyses to account for other known parameters uncertainties and for possible different model assumptions. As an example we recall that for the SD form factor an universal formulation is not possible since the internal degrees of the WIMP particle model (e.g. supersymmetry in case of neutralino) cannot be completely separated from the nuclear ones. In the calculations presented here we have adopted the SD form factors of ref. [18] estimated by considering the Nijmengen nucleon-nucleon potential. Other formulations are possible for SD form factors and can be considered with evident implications on the obtained allowed regions.

In conclusion, this analysis has shown that the DAMA data of the four annual cycles, analysed in terms of WIMP annual modulation signature, can also be compatible with a mixed scenario where both $\xi\sigma_{SI}$ and $\xi\sigma_{SD}$ are different from zero.

3.3 Inelastic Dark Matter

It has been suggested [19] that the observed annual modulation effect could be induced by possible inelastic Dark Matter: relic particles that prefer to scatter

inelastically off of nuclei. The inelastic Dark Matter could arise from a massive complex scalar split into two approximately degenerate real scalars or from a Dirac fermion split into two approximately degenerate Majorana fermions, namely χ_+ and χ_-, with a δ mass splitting. In particular, a specific model featuring a real component of the sneutrino, in which the mass splitting naturally arises, has been given in ref. [19]. It has been shown that for the χ_- inelastic scattering on target nuclei a kinematical constraint exists which favours heavy nuclei (such as ^{127}I) with respect to lighter ones (such as e.g. ^{nat}Ge) as target-detectors media. In fact, χ_- can only inelastically scatter by transitioning to χ_+ (slightly heavier state than χ_-) and this process can occur only if the χ_- velocity is larger than $v_{thr} = \sqrt{\frac{2\delta}{m_{WN}}}$ where m_{WN} is the WIMP-nucleus reduced mass ($c = 1$). This kinematical constraint becomes increasingly severe as the nucleus mass, m_N, is decreased [19]. Moreover, this model scenario gives rise – with respect to the case of WIMP elastically scattering – to an enhanced modulated component, S_m, with respect to the unmodulated one, S_0, and to largely different behaviours with energy for both S_0 and S_m (both show a higher mean value) [19].

A dedicated energy and time correlation analysis of the DAMA annual modulation data has been carried out [11] handling aspects other than the interaction type as in ref. [10] (in this way a particular model framework is fixed).

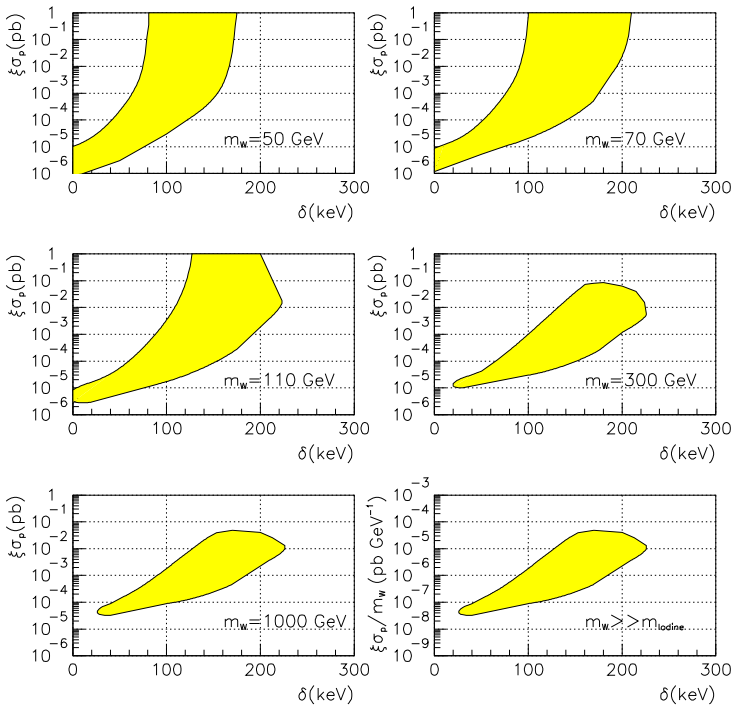

Fig. 5. An inelastic case: slices at fixed WIMP masses of the volume allowed at 3 σ C.L. in the space ($\xi\sigma_p$, δ, m_W) obtained for the model framework considered in ref. [11]; some of the uncertainties on used parameters have been included [11]. Note that e.g. Ge experiments cannot explore most of the DAMA allowed regions in this scenario.

In this scenario of Dark Matter with inelastic scattering an allowed volume in the space ($\xi\sigma_p$,m_W,δ) is obtained [11]. For simplicity, Fig. 5 shows slices of such an allowed volume at some given WIMP masses (3 σ C.L.). It can be noted that when $m_W \gg m_N$, the expected differential energy spectrum is trivially dependent on m_W and in particular it is proportional to the ratio between $\xi\sigma_p$ and m_W; this particular case is summarized in the last plot of Fig. 5. The allowed regions have been obtained – as in the previous cases – by the superposition of those obtained when varying the values of the previously mentioned parameters according to their uncertainties. Note that – as in the previous cases – each set of values (within those allowed by the associated uncertainties) for the previously mentioned parameters gives rise to a different expectation, thus to different "most likely" values. As an example we mention that when fixing the other parameters as in Ref. [10], the "most likely" values for a WIMP mass of 70 GeV are: i) $\xi\sigma_p = 2.5 \times 10^{-2}$ pb and $\delta = 115$ keV when $v_0 = 170$ km/s, ii) $\xi\sigma_p = 6.3 \times 10^{-4}$ pb and $\delta = 122$ keV when $v_0 = 220$ km/s; they are in δ region were Ge and Si experiment are disfavoured. Finally, we note also here that significant enlargement of the given allowed regions should be expected when including complete effects of model (and related experimental and theoretical parameters) uncertainties.

4 Proofs and Disproofs

Let us preliminary remark that the claim for contradiction made by some authors (see e.g. [20,21]) which use Ge target nuclei and different methodological approach is intrinsecally wrong. In fact (besides the usual uncertainties which always exist in the comparison of results achieved by different experiments): i) the annual modulation signature gives a model independent evidence for WIMPs independently on their nature and coupling, while an exclusion plot is always model dependent; thus, no direct and model-independent comparison can be pursued among experiments which use different approaches, different techniques and, even more, different target nuclei; ii) within the same general assumptions for a model e.g. SI coupling and isothermal halo, the proper accounting for parameters uncertainties, scaling laws uncertainties etc. significantly extends the allowed region and moves the best fit values; iii) there exist many model frameworks to which Na and I are sensitive and other nuclei (e.g. Ge and Si) are not. For example, a possible WIMP with a SI cross section of few 10^{-7} pb and with SD cross section of few 10^{-1} pb would produce a sizeable signal in DAMA but almost nothing in Ge and Si experiments. Moreover, also the given exclusion plots have a relative meaning since they are calculated under many assumptions; thus, they can drastically change either from model to model or just changing the value of each used experimental and theoretical parameter within its uncertainty.

Let us shortly remind that some comments about other discussions of purely SD component as well as about the comparisons with other direct and indirect experiments can be found in ref. [10]. Here, we only remind that the HEAT balloon experiment has confirmed an excess of high energy positrons in cosmic

rays which - if interpreted in terms of WIMP annihilation in a given particular scenario - gives rise to a result compatible with that of DAMA within the uncertainties (see e.g. [22]).

In the following only few comments on the CDMS-I result and on its comparison with that of DAMA are given.

As a general comment on the CDMS-I data [20] as well as on their re-analysis in [21], the arguments of our ref. [23] still hold. In addition, among the many crucial items necessary to credit the result itself and which are still missing, we cite: i) the measured energy spectra of gamma and electrons sources in running conditions. This can allow to show in a direct and safe way the detectors' response (from the peak positions and widths) and to derive the bulk detection efficiency; ii) the systematics associated to the used procedures since the measured counting rate is 60 counts keV^{-1} kg^{-1} d^{-1} (about 60 $\times$ 90keV $\times$ 15.8 kg $\times$ day = 85000 events, for the considered selected data sample) and only few of them (23 in the re-analysis) survive the veto, the so-called "quality cuts" (made - as mentioned in ref. [21] - to remove large periods with hardware troubles) and the discrimination. In addition, these few events are mainly discarded by means of a neutron background modelling which suffers of some flaws, e.g.: a) the systematics due to the large amount of so-called "surface events" present in all the regions of the discrimination plot for the Si data (as shown by CDMS so far and now not included in Fig. 40 of [21]); b) the uncertainties in the calculations based on the multiple scattering events. In fact, 4 events with both ionization yields Y1 and Y2 < 0.5 (that is neutron candidates) and about 60-70 events with Y1,Y2 about 1 (that is gamma/electron candidates) have been counted. The small number of gamma/electron multiple scattering has to be compared with the number of gamma/electron single scattering (after veto reduction procedure about 2 keV^{-1} kg^{-1} d^{-1} $\times$ 90keV $\times$ 15.8 kg $\times$ day = 2800 events). This is a relevant point since the neutron background modelling is based on the comparison of events with Y$<$0.5: 4 multiple-scatterings versus 23 single-scatterings.

Furthermore, let us quickly comment about the comparison that generally is done - see e.g. [21] - with the DAMA result.

As mentioned above in many models Ge and Si target nuclei are insensitive to WIMP candidate to which instead Na and I are. Furthermore, in the models where all of them are sensitive, in order to obtain cross-section limits/regions from the experimental data, it is necessary to assume an astrophysical, particle and nuclear Physics model framework, to define a set of parameters values and to scale the cross sections on the different target nuclei to the one on proton. Therefore, every inferred result strongly depends e.g. on the chosen model, on the set of values fixed for the experimental and theoretical parameters and on the scaling laws for each involved nucleus. Thus, large uncertainty is associated to the results. This is a crucial point that must be accounted every time a comparison among results from different experiments and with theoretical models is attempted, avoiding that a reader might have the wrong idea of the "universality" of the conclusion.

In particular, as regards the purely spin-independent coupled WIMPs, which is practically the only scenario considered by other authors, the comparisons are often arbitrarily performed not with the region correctly endorsed by the DAMA collaboration (that is including the constraint from the measured upper limits) for the given simplified model framework of ref. [8] (see again [21]). In fact, as an example, in Fig. 6 the exclusion limits claimed by CDMS and EDELWEISS are superimposed to the correct DAMA region for the simplified model with isothermal galactic halo, "simple" scaling laws and fixed assumptions for all the parameters as in ref. [8], but assuming here the v_0 value at 220 km/s (that is neglecting the effect of its existing uncertainty on the allowed region, as correctly accounted in ref. [8] and here in the previous fig. 2).

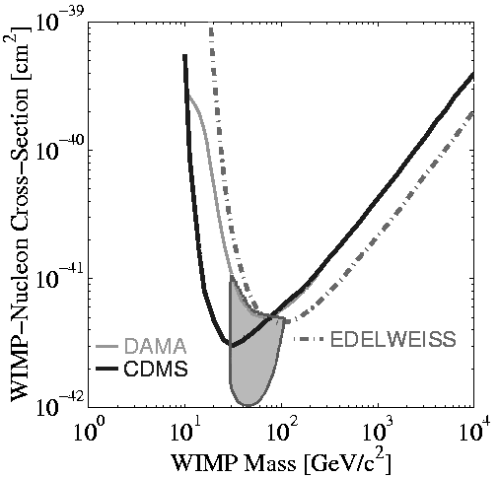

Fig. 6. A model dependent comparison for purely SI coupled WIMP: exclusion limits claimed by CDMS [21] and EDELWEISS [24], superimposed to the DAMA region allowed in the simplified model with isothermal galactic halo, "simple" scaling laws and fixed assumptions for all the parameters; in particular, here, for the comparison v_0 has been set to the value 220 km/s (that the effect of its existing uncertainty on the allowed region - correctly accounted in ref. [8] and here in the previous fig. 2 - has been neglected). This figure is as in ref. [21], but here the correct region allowed by the cumulative DAMA data under the mentioned assumptions is shown. We further remind that the proper inclusion of the existing models' uncertainties significantly enlarges the allowed region (see e.g. the case of inclusion of v_0 uncertainties and of halo modelling in Fig. 2 and 3, respectively). Also exclusion plots do not show "universal" boundary, but are affected by large experimental and theoretical uncertainties.

Moreover, in ref. [21] a comparison is pursued by using some "most likely" values quoted in ref. [8]; however, it is worth to note that these "most likely" values have not a general validity, but depend on the specific assumptions (on halo, on particle, on nuclear physics) and experimental (e.g. quenching factors, detector response, etc.) and theoretical (form factors, scaling laws, etc.) parameters' values. Varying them within the existing uncertainties varies the "most

likely" values. Realistic estimates of the expected number of counts in CDMS-I from the DAMA results for the purely SI coupled WIMPs can vary from about 20 down to about 1. Moreover, let us remind that - even under the unrealistic assumption of no systematics in the hardware and software CDMS data reduction - the calculated exclusion plot has not an "universal" validity.

A comparison between the Ge result and a particular model dependent extrapolation from the DAMA 2-6 keV cumulative residuals has also been addressed in ref. [21]; this is again model dependent and, in particular, depends on the used quenching factors, form factor parameters, etc. In particular, the used procedures does take into account neither the energy behaviour of the measured modulation amplitude and the upper limits on recoils nor the proper values and uncertainties of parameters needed in the calculation. Thus, considerations similar to the previous case hold.

Finally, in Fig. 47 of ref. [21] – as sometimes happens in other presentations – the theoretical expectations for the particular case of the neutralino are shown without taking into account the uncertainties on the local halo density and the rescaling procedures (as well as on some other astrophysical, nuclear and particle physics aspects). This incorrect procedure leads to wrong conclusion.

Summarizing, there is no solid scientific reason for the CDMS claim for contradiction whatever scenario would be considered.

5 Towards LIBRA

At present our main efforts are devoted to the realization of LIBRA (Large sodium Iodine Bulk for RAre processes in the DAMA experiment) consisting of $\simeq$ 250 kg of NaI(Tl). New radiopure detectors by chemical/physical purification of NaI and Tl powders as a result of a dedicated R&D with Crismatec have been realized. The installation of this set-up is foreseen in fall 2002; this will allow us to increase the sensitivity of the experiment. Some related arguments can be found in ref. [25].

6 Conclusions

The DAMA annual modulation data of four annual cycles [4,6,7,8,9,10,11] have been analysed by energy and time correlation analysis in terms of purely SI, purely SD, mixed SI/SD, "preferred" inelastic WIMP scattering model frameworks.

To effectively discriminate among the different possible scenarios further investigations are in progress. In particular, the data of the 5^{th} and 6^{th} annual cycles are at hand, while the set-up is running to collect the data of a 7^{th} annual cycle. Moreover, the LIBRA (Large sodium Iodine Bulk for RAre processes) set-up is under construction to increase the experimental sensitivity.

References

1. P. Belli et al., *Astrop. Phys.* **5** (1996) 217; P. Belli et al., *Il Nuovo Cimento* **C 19** (1996) 537; P. Belli et al., *Phys. Lett.* **B 387** (1996) 222 and *Phys. Lett.* **B 389** (1996) 783(err.); R. Bernabei et al., *Astrop. Phys.* **7** (1997) 73; R. Bernabei et al., *Il Nuovo Cimento* **A 110** (1997) 189; R. Bernabei et al., *Phys. Lett.* **B 408** (1997) 439; R. Bernabei et al., *Phys. Lett.* **B 436** (1998) 379; P. Belli et al., *Astrop. Phys.* **10** (1999) 115; P. Belli et al., *Phys. Lett.* **B 460** (1999) 236; P. Belli et al., *Nucl. Phys.* **B 563** (1999) 97; R. Bernabei et al., *Phys. Rev. Lett.* **83** (1999) 4918; P. Belli et al., *Phys. Rev.* **C 60** (1999) 065501; P. Belli et al., *Phys. Lett.* **B 465** (1999) 315; P. Belli et al., *Phys. Rev.* **D 61** (2000) 117301; R. Bernabei et al., *New Journal of Physics* **2** (2000) 15.1, (www.njp.org); R. Bernabei et al., *Phys. Lett.* **B 493** (2000) 12; R. Bernabei et al., *Nucl. Instr. & Meth.* **A482** (2002) 728; R. Bernabei et al., *Phys. Lett.* **B 515** (2001) 6; R. Bernabei et al., *Eur. Phys. J. direct* **C 11** (2001) 1; R. Bernabei et al., *Phys. Lett.* **B 527** (2002) 182; R. Bernabei et al., *Nucl. Phys.* **A 705** (2002) 29; R. Bernabei et al., INFN/AE-01/19, to appear on XENON-01, World Sci. Pub.
2. R. Bernabei et al., *Il Nuovo Cimento* **A 112** (1999) 1541
3. R. Bernabei et al., *Phys. Lett.* **B 389** (1996) 757
4. R. Bernabei et al., *Phys. Lett.* **B 424** (1998) 195
5. R. Bernabei et al., *Il Nuovo Cimento* **A 112** (1999) 545
6. R. Bernabei et al., *Phys. Lett.* **B 450** (1999) 448
7. P. Belli et al., *Phys. Rev.* **D 61** (2000) 023512
8. R. Bernabei et al., *Phys. Lett.* **B 480** (2000) 23
9. R. Bernabei et al., *Eur. Phys. J.* **C 18** (2000) 283
10. R. Bernabei et al., *Phys. Lett.* **B 509** (2001) 197
11. R. Bernabei el al., *Eur. Phys. J.* **C 23** (2002) 61
12. P. Belli et al., hep-ph/0203242
13. N.J.C. Spooner, Pub. Boston, "Particles, Strings and Cosmology" (1998) 130
14. K.A. Drukier et al., *Phys. Rev.* **D 33** (1986) 3495; K. Freese et al., *Phys. Rev.* **D 37** (1988) 3388
15. A. Bottino et al., *Phys. Lett.* **B 402** (1997) 113; *Phys. Lett.* **B 423** (1998) 109; *Phys. Rev.* **D 59** (1999) 095004; *Phys. Rev.* **D 59** (1999) 095003; *Astrop. Phys.* **10** (1999) 203; *Astrop. Phys.* **13** (2000) 215; *Phys. Rev.* **D 62** (2000) 056006; hep-ph/0010203; hep-ph/0012377
16. R.W. Arnowitt and P. Nath, *Phys. Rev.* **D 60** (1999) 044002; E. Gabrielli et al., hep-ph/0006266
17. D. Fargion et al., *Pis'ma Zh. Eksp. Teor. Fiz.* **68**, (*JETP Lett.* **68**, 685) (1998); *Astrop. Phys.* **12** (2000) 307
18. M.T. Ressell et al., *Phys. Rev.* **C 56** (1997) 535
19. D. Smith and N. Weiner, *Phys. Rev.* **D 64** (2001) 043502
20. CDMS collaboration, *Phys. Rev. Lett.* **84** (2000) 5699
21. CDMS collaboration, astro-ph/0203500
22. G.L. Kane et al., hep-ph/0108138
23. P. Belli et al., in the volume "Relativistic Astrophysics", 20th Texas Symp., AIP (2001) 95; pre-print available on DAMA homepage on http://www.lngs.infn.it
24. EDELWEISS collaboration, *Phys. Lett.* **B 513** (2001) 15
25. R. Bernabei, *Prog. Part. Nucl. Phys.* **48** (2002) 263